Adsorption 7: 249–264, 2001

On the Application of Various Methods to Evaluate the Microporous Properties of Activated Carbons

S.A. KORILI* AND A. GIL†
Departamento de Química Aplicada, Edificio Los Acebos, Universidad Pública de Navarra, 31006 Pamplona, Spain

Received December 11, 2000; Revised July 27, 2001; Accepted July 27, 2001

Abstract. Three methods, the Horvath-Kawazoe (HK) method, the Jaroniec-Gadkare-Choma (JGC) one and the Density Functional Theory (DFT), have been applied in the characterization of the microporous structure of several activated carbons. The samples were all based on the same parent material, that was subjected to various oxidative treatments, using solutions of concentrated HNO_3 at various temperatures (298, 333, 363 and reflux at 383 K during 3 hours) or solutions of H_2O_2 of various concentrations (1, 5 and 10 M). The nitrogen adsorption isotherms of the solids, were studied at 77 K and in the relative pressure range of $10^{-6} < p/p^0 < 0.99$. Only the isotherm parts up to a relative pressure of 0.2 were taken into consideration for obtaining the micropore size distributions. The evaluation of the method suitability was based on how well each one describes the experimentally obtained data. The three methods describe satisfactorily the experimental results, including the transitions of the isotherms related to the stages of micropore filling. The effects of the oxidative treatment on the structure of the solids, as judged from their micropore size distributions, are also discussed.

Keywords: activated carbon, micropore size distribution, Horvath-Kawazoe model, Jaroniec-Gadkare-Choma model, density functional theory

1. Introduction

Activated carbons are widely used as adsorbents and supports for heterogeneous catalysts because their porosity and surface chemistry can be controlled, and because of their relatively low reactivity. The functional groups present on the carbon surface have a strong influence on the performance of these materials as supports for metallic catalysts (De la Puente et al., 1998, 1999; Derbysshire et al., 1986; Ehrburger et al., 1976; Gandía and Montes, 1994; Kim et al., 1993; Martín-Gullón et al., 1993; Prado-Burguete et al., 1991; Román-Martínez et al., 1995; Suh et al., 1993; Vissers et al., 1987) and other, non-catalytic applications (Bautista-Toledo et al., 1994). Several methods have been reported in the literature to generate surface carbon-oxygen complexes, and can be classified into two broad categories: methods involving reactions with oxidizing gases and the ones involving reactions with oxidizing solutions (Puri, 1970). The intention is to create oxygen functionalities while producing only minimum changes to the structural properties, mainly in the microporous region (Bautista-Toledo et al., 1994; Gil et al., 1997). The thermal conditions when using oxidizing solutions are milder and they are recommended when the presence of surface oxygen has to be preserved.

In order to characterize the structure of the materials, that is to obtain the pore size distribution, as well as the specific surface area and the adsorption energy distribution, several classic or novel adsorption models are reported in the literature (Carrot et al., 1988; Dollimore

*On leave from Aristotle University of Thessaloniki, Greece.
†To whom correspondence should be addressed.
andoni@unavarra.es

and Heal, 1964; Horvath and Kawazoe, 1983; Jaroniec and Choma, 1988; Jaroniec et al., 1996; Mikhail et al., 1968; Parent and Moffat, 1995; Russell and LeVan, 1994; Seaton et al., 1989). Historically, the Kelvin (Gregg and Sing, 1991) equation of classic thermodynamics has been first used to relate the pore width to the filling pressure. This equation is restricted to pore sizes greater than 2 nm, as it does not take into account the thickness of the adsorbate layers formed on the porous surface prior to condensation. Various methods (De Boer et al., 1965; Everett and Ottewill, 1970; Lecloux and Pirard, 1979; Zhu et al., 1997) account for film growth, by coupling the Kelvin equation with a standard isotherm, the t-curve, which describes the thickness of the precondensate film. However, these models neglect the large potential enhancement in narrow pores, where adsorbed molecules are proximate to both surfaces and the adsorbed films on opposing walls interact. Therefore, the models based on the Kelvin equation and the standard isotherm, overestimate the pressures at which film wetting and capillary condensation occur. Thus, they are unreliable for pore size distribution interpretation below about 7.5 nm.

The information about the presence of fine pores is crucial for understanding the adsorption and catalytic properties of many porous solids, and therefore numerous characterization methods were developed to obtain micropore size distributions. One semi-empirical approach is to combine the Dubinin equations for the micropore volume estimation with a gamma-type distribution (Jaroniec et al., 1988, 1989, 1991; Stoeckli, 1977). Horvath and Kawazoe (1983) provided a simple method for the calculation of the effective pore size distribution using the slit potential model developed by Everett and Powl (1976). This method gives a simple one-to-one correspondence between the pore size and the relative pressure at which the pore is filled. Recently, improved HK equations have also been proposed (Cheng and Yang, 1994) and an equivalent procedure based on the adsorption potential distribution has been developed by Jaroniec et al. (1996). These approaches were developed for slit-like pores and extended to spherical and cylindrical ones (Baksh and Yang, 1991; Saito and Foley, 1991, 1995a, 1995b). The HK method has been widely applied to characterize various microporous solids as pillared interlayered clays (Baksh and Yang, 1992; Brandt and Kydd, 1997; Cañizares et al., 1999; Ge et al., 1994; Gil and Montes, 1994; Gil et al., 1995; Gil and Grange, 1997; Hutson et al., 1999; Malla and Komarneni, 1993; Storaro et al., 1996) and activated carbons (Foley, 1995; Rychlicki et al., 1993), as the slit-like model is a good representation of the pore structures of the above materials. Some problems related to the interpretation of the HK distributions have also been presented and discussed by various authors (Kruk et al., 1997, 1998; Webb and Orr, 1997). However, the HK results must be combined with a Kelvin-type method to describe the full pore size distribution.

The most promising, but unfortunately the most complicated and model-dependent methods for evaluating micropore size distributions, are based on advanced computational techniques, which provide reliable local isotherms for pores of well-defined geometry. Several authors (Do and Do, 1995; Heuchel and Jaroniec, 1995a, 1995b; Jaroniec and Kaneko, 1997; Nicholson, 1994; Suzuki et al., 1996) have used computer simulations, such as molecular dynamics and Monte Carlo methods, to predict the adsorption isotherms and the thermodynamic properties of various adsorbates on molecular sieves. With these methods, it is not necessary to have an analytical expression for the adsorption isotherm in order to obtain information from experimental data. An alternative to the computer simulation techniques is given by the density functional theory. Seaton et al. (1989) used the density functional theory as the basis of a practical method for determining the pore size distribution of carbons. Olivier et al. (1994) extended and generalized the method by numerical deconvolution of the distribution which results from the data and a set of model isotherms covering a wide range of pore sizes, from 0.4 to 400 nm. Various density approximations (Olivier et al., 1994; Lastoskie et al., 1993a) have been used in order to predict the isotherms for slit-shaped pores. In the following, these methods are briefly presented.

2. Theoretical Approach

2.1. The Horvath-Kawazoe (HK) Model

Everett and Powl (1976) showed that the potential energy of interaction, ε, between one adsorbate molecule and two parallel lattice planes whose nuclei are separated by a distance x apart, can be expressed via the Lennard-Jones (12:6) potential. Therefore, for a slit pore filled with adsorbate molecules, ε can be written

as follows:

$$\varepsilon = \frac{N_a A_a + N_A A_A}{2\sigma^4}\left[-\left(\frac{\sigma}{z}\right)^4 + \left(\frac{\sigma}{z}\right)^{10} - \left(\frac{\sigma}{x-z}\right)^4 + \left(\frac{\sigma}{x-z}\right)^{10}\right] \quad (1)$$

where

$$\sigma = \left(\frac{2}{5}\right)^{1/6} d_0 \quad (2)$$

where d_0 is the arithmetic mean diameter of the adsorbate molecule and the adsorbent atom, z is the displacement of a molecule from the plane of surface nuclei (one plate), N_a is the number of oxide ions per unit area of surface, and N_A is the number of molecules of adsorbate per unit surface area of the adsorbate. A_a and A_A are the dispersion constants, which are given by the Kirkwood-Muller equations (Gregg and Sing, 1991) as follows:

$$A_a = \frac{6mc^2\alpha_a\alpha_A}{\frac{\alpha_A}{\chi_A} + \frac{\alpha_a}{\chi_a}} \quad (3)$$

and

$$A_A = \frac{3}{2}(mc^2\alpha_A\chi_A) \quad (4)$$

where m is the electron mass, c is the speed of light, α_a and χ_a are respectively the polarizability and magnetic susceptibility of an adsorbent atom, and α_A and χ_A are the polarizability and magnetic susceptibility of an adsorbate molecule. The sum $N_a A_a + N_A A_A$ is the so-called interaction parameter, that summarizes the physicochemical properties of the adsorbate-adsorbent system, which are not easily available. To overcome this difficulty, Gil and Grange (1997) proposed a new procedure for the calculation of this parameter, based on the best fitting of the micropore size distribution for an activated carbon and an alumina pillared clay, considering as upper limit of the micropore size a diameter of 2 nm. The value of the interaction parameter obtained by the authors was 45.74 cal · nm^4/mol.

According to Horvath and Kawazoe (1983), the free energy of adsorption is equal to the net energy of interaction between the layers. Thus, the following expression is derived for a slit-like geometry:

$$RT\ln\frac{p}{p^0} = N_{Av}\frac{N_a A_a + N_A A_A}{\sigma^4(x-2d_0)} \times\left[\frac{\sigma^4}{3(x-d_0)^3} - \frac{\sigma^{10}}{9(x-d_0)^9} - \frac{\sigma^4}{3d_0^3} + \frac{\sigma^{10}}{9d_0^9}\right] \quad (5)$$

where N_{Av} is Avogadro's number. It is assumed that the adsorbed phase was like a two-dimensional ideal gas, therefore the Henry's law can be applied. Recently, Cheng and Yang (1994) proposed a modification of this method, replacing the Henry's law used by Horvath and Kawazoe by a Langmuir-type equation. Both approaches have been applied and compared by Gil et al. (2000) in the characterization of the microporous properties of pillared interlayered clays, giving similar pore size distributions.

Taking into account the experimental results from nitrogen adsorption, volume adsorbed *versus* relative pressure, the pore size distribution can be derived from Eq. (5). The microporous volume is calculated as the adsorbed volume that corresponds to a pore size of 2 nm (Gil and Grange, 1997).

2.2. *The Jaroniec-Gadkare-Choma (JGC) Model*

Porous solids are usually energetically and structurally heterogeneous (Gil and Korili, 2000; Jaroniec, 1995). The energetic heterogeneity of solids is commonly characterized by the differential distribution of the amount adsorbed, V, with respect to the adsorption energy U (Jaroniec and Madey, 1988; Ross and Olivier, 1964):

$$F(U) = -\frac{dV}{dU} \quad (6)$$

where U is positive and defined as the minimum of the gas-solid potential taken with minus sign for a molecule contained in a fine pore (Everett and Powl, 1976). The structural heterogeneity of a porous solid is usually characterized by the differential distribution of V with respect to the pore width x (Gregg and Sing, 1991):

$$J(x) = \frac{dV}{dx} \quad (7)$$

According to Jagiello and Schwarz (1993) the relationship between these two types of distributions can

be expressed as:

$$J(x) = \frac{dV}{dx} = \frac{dV}{dU}\frac{dU}{dx} = -F(U)\frac{dU}{dx} \qquad (8)$$

The practical use of Eq. (8) to convert $F(U)$ to $J(x)$, or vice versa, is almost impossible for real solids, because the relation between U and x is determined not only by the size and shape of fine pores, which are the source of the structural heterogeneity, but also by the presence of various surface atoms, functional groups, impurities and irregularities, which reflect the energetic, that is surface and chemical, heterogeneity of the pore walls. This relation becomes much simpler for highly microporous solids, such as some microporous carbons. For this type of porous solids the adsorption energy U does not vary across the pore wall, but depends only on the micropore geometry and width, x, and $U(x)$ can be expressed analytically (Jagiello and Schwarz, 1993). In this case, it is necessary to obtain the energy distribution of surface molecules from experimental adsorption data.

Under this assumption of the condensation approximation (CA), Jaroniec et al. (1996) proposed a simple thermodynamic approach to characterize porous solids, and particularly to discuss the relation between the structural and energetic heterogeneities. A key thermodynamic quantity in this approach is the differential adsorption potential, which describes quantitatively all possible changes in the Gibbs free energy of a given gas-solid sorption system.

The adsorption potential A is equal to the change in the Gibbs free energy of adsorption with the minus sign:

$$A = -\Delta G = RT\ln\left(\frac{p^0}{p}\right) \qquad (9)$$

Here p^0 denotes the saturation vapor pressure and R is the universal gas constant. The plot of the amount of gas adsorbed, V, against the adsorption potential, A, adsorption curve, can be considered as the primary thermodynamic characteristic of the adsorption system studied. The differential adsorption potential distribution function $X(A)$ is defined as:

$$X(A) = -\frac{dV(A)}{dA} \qquad (10)$$

The pore volume distribution $J(x)$ can be related to the adsorption potential distribution through the following equation:

$$J(x) = \frac{dV}{dx} = \left(\frac{dV}{dA}\right)\left(\frac{dA}{dx}\right) = -X(A)\left(\frac{dA}{dx}\right) \qquad (11)$$

According to this last equation, the pore volume distribution $J(x)$ can be obtained by multiplication of the adsorption potential distribution by $-dA/dx$. This quantity depends on the pore range and pore geometry. In the case of slit-like micropores, the derivative of the adsorption potential A with respect to the pore width x can be found from the following relation between A and x (Jaroniec et al., 1996):

$$A = \frac{C_1}{(x - d_A)}\left[\frac{C_3}{(x + d_0)^9} - \frac{C_2}{(x + d_0)^3} + C_4\right] \qquad (12)$$

where the constants C_1, C_2, C_3, and C_4 are characteristic for a given adsorbent-adsorbate system. The symbol d_A denotes the diameter of the adsorbate molecule, and $d_0 = (d_a - d_A)/2$, where d_a is the diameter of the adsorbent atom. After differentiation with respect to the pore width x, the following expression is obtained:

$$\frac{dA}{dx} = \frac{C_1}{(x - d_A)}\left[\frac{3C_2}{(x + d_0)^4} - \frac{9C_3}{(x + d_0)^{10}}\right] - \frac{C_1}{(x - d_A)^2}\left[\frac{C_3}{(x + d_0)^9} - \frac{C_2}{(x + d_0)^3} + C_4\right] \qquad (13)$$

The values of the constants in Eq. (13) for nitrogen adsorption in slit-like carbonaceous micropores at 77 K are the following (Jaroniec et al., 1996): $C_1 = 39.60\,\text{kJ·nm/mol}$, $C_2 = 1.89 \times 10^{-3}\,\text{nm}^4$, $C_3 = 2.70 \times 10^{-7}\,\text{nm}^{10}$, $C_4 = 0.050$ nm, and $d_A = 0.30$ nm. The adsorption isotherm data allow to obtain the differential adsorption potential distribution $X(A)$ (Gil and Grange, 1996), which, after multiplication by (dA/dx) from Eq. (13) and change of the sign, leads to the pore volume distribution $J(x)$.

2.3. *Density Functional Theory (DFT)*

The mean field density functional theory method, proposed by Seaton et al. (1989), is a novel statistical mechanical attempt to extend the accuracy of pore size distribution analysis in both the mesopore and micropore range.

The adsorption equilibrium isotherm can be used to provide information about the structural and the

energetic heterogeneity of a given adsorbate-adsorbent system. In mathematical terms, the adsorption isotherm of a single component can be expressed by the following integral equation:

$$X(p) = \int f(x)\varphi(p, x)\, dx \qquad (14)$$

where $X(p)$ is the experimental isotherm, $\varphi(p, x)$ is the mean density of the adsorbate in a pore of width x at pressure p, and $f(x)$ is the pore size distribution of the adsorbent.

The density functional theory provides a set of model isotherms $\varphi(p, x)$ for homogeneous pores of given sizes, which are then applied to the experimental adsorption measurements in the numerical solution of Eq. (14) to obtain the pore size distribution $f(x)$.

In this method, the adsorbent-adsorbate properties are chosen to provide the best fit to the experimental nitrogen adsorption data on a homotattic graphite (Olivier et al., 1994). The interaction potential parameters used have been obtained from the literature (Lastoskie et al., 1993b).

In this work, the microporous texture evolution of an activated carbon modified with HNO_3 or H_2O_2 liquid-phase oxidation treatments has been studied. The three presented methods, the Horvath-Kawazoe, the Jaroniec-Gadkare-Choma and the Density Functional Theory, have been applied to the nitrogen adsorption at 77 K in order to evaluate the effect of the treatments on the porosity of the solids.

3. Experimental

The material used in this study, referred hereafter as sample K0, was a commercial granular microporous gas-activated carbon based on coconut shell (Merck-9631). A series of samples of this carbon was subjected to oxidative treatments with concentrated HNO_3 (Janssen Chimica) at various temperatures, namely 298, 333, and 363 K and reflux at 383 K, during 3 h. These modified samples are referred as N298, N333, N363, and NR, respectively. Another series of carbon samples was treated with H_2O_2 of various concentrations, 1, 5 and 10 M, at 363 K during 5 h. These samples are referred as C1, C5, and C10, respectively. Details of the oxidative treatments are given elsewhere (Gil et al., 1997).

The structural characterization of the activated carbons was made by nitrogen adsorption at 77 K, using a static volumetric apparatus (Micromeritics ASAP 2000M adsorption analyzer). The adsorption isotherms were obtained in the relative pressure range of $10^{-6} < p/p^0 < 0.99$, using 0.1 g of sample. At the beginning of each adsorption experiment, successive doses of 5 cm^3 (STP) of nitrogen per catalyst gram, were fed to the sample, until $p/p^0 = 0.04$ was reached. After this point, nitrogen was added to achieve a fixed set of p/p^0 values, and the required volumes were measured. Before the analysis, the activated carbons were degassed at 473 K during 10 h, at a pressure not exceeding 10^{-3} mmHg.

Specific total surface areas (S_{Lang}) were calculated using the Langmuir equation ($0.01 \leq p/p^0 \leq 0.05$, interval of p/p^0) for monolayers. Specific external surface areas (S_{ext}) were obtained from the t method (Lippens and de Boer, 1965), and the specific total pore volumes (V_{p}) were estimated from the nitrogen uptake at $p/p^0 = 0.95$. The Dubinin-Astakhov (DA) equation (Dubinin, 1975) has been applied to obtain the micropore volume, V_{DA}, and the characteristic energy, E, from the plot of $\log^n(p^0/p)$ versus $\log V$. The n exponents of the DA equation were calculated by linear regression, in the range of relative pressures of $2 \times 10^{-6} \leq p/p^0 \leq 0.2$.

4. Results and Discussion

The nitrogen adsorption at 77 K of the modified activated carbons is shown in Figs. 1 and 2. All the adsorption isotherms are of type I in the Brunauer, Deming, Deming, and Teller (BDDT) classification (Gregg and Sing, 1991). From these figures, it can be seen that

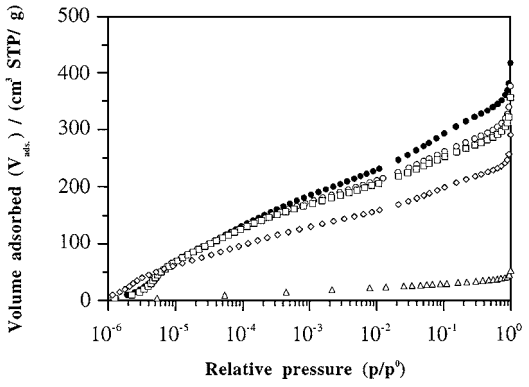

Figure 1. Nitrogen adsorption at 77 K starting from very low pressures of the activated carbon samples treated with HNO_3, (●) K0, (○) N298, (□) N333, (◇) N363 and (△) NR.

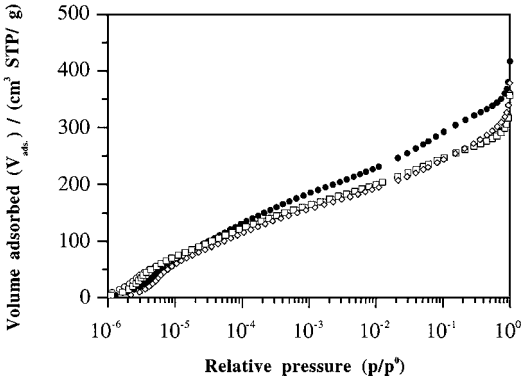

Figure 2. Nitrogen adsorption at 77 K starting from very low pressures of the activated carbon samples treated with H_2O_2. (●) K0, (○) Cl, (□) C5, and (◇) C10.

treatments with HNO_3 and H_2O_2 affect in general both the microporous and the mesoporous regions. The majority of differences among the various samples can be observed at low relative pressures, at $p/p^0 < 0.2$. In this region, micropore filling takes place, with the interaction of nitrogen with the micropore surface being stronger than that with the adsorption sites on the solid surface. Various stages of micropore filling occur, related to the different micropore structures. The low-pressure region of the nitrogen adsorption in general corresponds to two stages of micropore filling (Sing, 1989): an initial process, at $p/p^0 < 0.005$, that takes place in pores having dimensions comparable to nitrogen molecule, called ultramicropores, and a molecule interaction process that occurs at p/p^0 higher than 0.005 (0.005–0.2). In this latter relative pressure range, it is also possible to consider the filling of two micropore ranges, referred as micropores and supermicropores (Kakei et al., 1990), which occurs at the relative pressure ranges of 0.005–0.08 and 0.08–0.2, respectively.

The nitrogen adsorption at 77 K of the activated carbons treated with solutions of concentrated HNO_3 is shown in Fig. 1. When the nitrogen adsorption of the starting activated carbon and that of the samples N298 and N333 are compared, it can be seen that the oxidation treatment affected mainly the region from $p/p^0 = 4 \times 10^{-4}$ to $p/p^0 = 1$, that is the one corresponding to the micropores, supermicropores and mesopores. For these samples, no differences are observed for relative pressures lower than 10^{-4}. The nitrogen adsorption at 77 K for sample N363 shows the creation of ultramicropores in this pressure range. A partial loss of the rest of the pores, micropores and mesopores, is also observed. Finally, the reflux treatment produces an almost total loss of the porosity of the activated carbon.

The nitrogen adsorption at 77 K of the activated carbons treated with solutions of H_2O_2 is shown in Fig. 2. For samples C1 and C5, a development of ultramicropores and a loss of mesoporous volume is observed, while sample C10 shows a continuous loss of pore volume in the overall pressure range. Differences mainly in the ultramicropore region can be detected from a comparison of the nitrogen adsorption of these samples.

The structural properties are more explicitly given in Table 1, where the specific surface areas, S_{Lang} and S_{ext}, and the specific pore volumes, V_{p} and V_{DA}, of all the samples are presented. The treatment with solutions of concentrated HNO_3 produces a loss of the structural properties of the activated carbon, that becomes more pronounced as the treatment temperature increases. In fact, the structural properties change only a little when the starting activated carbon is treated with HNO_3 at 298 and 333 K. Under these conditions, and considering the starting material as reference, the loss in the specific surface area and specific pore volume is as low as 4–16%. The treatment of sample K0 at a higher temperature, 363 K, brings about a loss of 32–37% of the specific surface areas and 33–43% of the specific pore volumes. The losses are increased up to 83–90% when the activated carbon is treated under reflux. On the other hand, the structural properties remain nearly the same when the activated carbon is treated with H_2O_2. The treatment with solutions of H_2O_2 1M (sample C1) produces the loss of 10–18% of the specific surface areas and the specific pore volumes. These losses are similar to those of the other samples (C5 and C10), treated with solutions of higher concentrations.

It has been reported that the reaction of activated carbon with solutions of HNO_3 and H_2O_2 changes not only the chemical nature of its surface by the presence of several types of oxygen surface groups, but also its structural characteristics (De la Puente et al., 1997, 1998; Gil et al., 1997). By the use of solutions of concentrated HNO_3 at low temperatures, as with samples N298 and N333, the fixation of oxygen groups on the walls of mesopores (Bautista-Toledo et al., 1994) gives rise to a decrease of pore size, and therefore a decrease of the mesopore volume. Upon oxidation at higher temperature (sample N363), more oxygen groups are fixed, decreasing further the size of the pores and converting those previously classified as mesopores into micropores. The treatment under reflux conditions leads to an

Table 1. Structural properties of the modified activated carbons.

					HK model		JGC model	DFT model	
Sample	S_{Lang}[a,b]	V_p[c]	S_{ext}[a]	V_{DA}[d]	$V_{\mu pHK}$[e]	dp_{HK}[f]	dp_{JGC}[g]	$V_{\mu pDFT}$[h]	dp_{DFT}[i]
K0	1242 ($C^j = 333$)	0.589	70	0.481	0.486	0.48 (0.60)	0.49	0.360	0.64
N298	1116 ($C = 365$)	0.525	67	0.422	0.429	0.48 (0.50)	0.49	0.316	0.59
N333	1075 ($C = 391$)	0.498	59	0.406	0.413	0.48 (0.50)	0.48	0.307	0.59
N363	842 ($C = 358$)	0.397	44	0.273	0.330	0.46 (0.55)	0.49	0.260	0.59
NR	129 ($C = 269$)	0.070	12	0.055	0.051	0.56	0.56	0.039	0.80
C1	1055 ($C = 373$)	0.498	63	0.412	0.407	0.47 (0.53)	0.48	0.316	0.59
C5	1052 ($C = 414$)	0.491	60	0.403	0.405	0.47	0.48	0.312	0.59
C10	1035 ($C = 350$)	0.526	73	0.396	0.408	0.48 (0.55)	0.49	0.305	0.59

[a]Specific surface area in m^2/g.
[b]$0.01 \leq p/p^0 \leq 0.05$, interval of p/p^0.
[c]Specific total pore volume at $p/p^0 = 0.95$ in cm^3/g.
[d]Specific micropore volume from Dubinin-Astakhov formalism in cm^3/g.
[e]Specific micropore volume derived from the Horvath-Kawazoe model in cm^3/g.
[f]Maximum pore diameter of the Horvath-Kawazoe micropore size distribution in nm. The shoulder pore diameter is given in the brackets.
[g]Maximum pore diameter of the Jaroniec-Gadkare-Choma micropore size distribution in nm.
[h]Specific micropore volume derived from the DFT model in cm^3/g.
[i]Principal maximum pore diameter of the DFT pore size distribution in nm.
[j]Langmuir C-value, characteristic of the intensity of the adsorbate-adsorbent interactions.

almost complete loss of the porosity of the activated carbon. Together with the process of oxygen fixation, this indicates that some pores were destroyed because of the loss of pore walls. The treatment with solutions of H_2O_2 at low concentrations, 1 and 5 M, allows the fixation of oxygen groups decreasing the size of the pores in a similar way to the previously described in the treatment with HNO_3, sample N363. At a higher concentration of H_2O_2, 10 M, a little loss of the microporosity of the activated carbon is observed, while the structural characteristics remain practically unchanged.

The micropore size distributions of the samples, derived from the slit-like model of Horvath and Kawazoe, are shown in Fig. 3. The distributions confirm the results obtained from the nitrogen adsorption at 77 K and presented in Figs. 1 and 2. The presence of a maximum and a shoulder are in accordance with the transitions observed in the isotherms. The microporous volumes, calculated as proposed by Gil and Grange (1997), were also included in Table 1, and it can be seen that an excellent agreement exists between the values obtained with the HK and DA approaches. When the micropore distributions of the starting activated carbon and those of the samples N298 and N333 are compared (see Fig. 3), no differences are observed. The distributions show a maximum, at about 0.48 nm, and a shoulder. The pore diameter related with each shoulder is shown in Table 1. The distribution for sample N363 shows a shift of the maximum, from 0.48 to 0.46 nm. With these samples, treated with concentrated HNO_3, a loss of micropore volume is observed, ranging from 12 to 90% and increasing as the thermal treatment temperature increases. The reflux treatment produces a total loss of the microporosity of the activated carbon. When the micropore distributions of the starting activated carbon and those of the samples C1 and C5 are compared (see Fig. 3), a shift of the maximum micropore diameter from 0.48 to 0.47 nm is observed. The distribution remains almost unchanged when the starting material is treated with H_2O_2 10 M (sample C10). The evolution of the specific micropore volume of these modified activated carbons, indicates that this property remains nearly unchanged when the activated carbon is treated with solutions of H_2O_2. This treatment brings about a loss of 16% of the specific micropore volume.

The micropore size distributions obtained with the JGC model, are shown in Fig. 4. Each of these distributions exhibits a distinct peak located at 0.48–0.49 nm (see Table 1). Except of this peak, the distributions are quite flat and no difference can be observed among

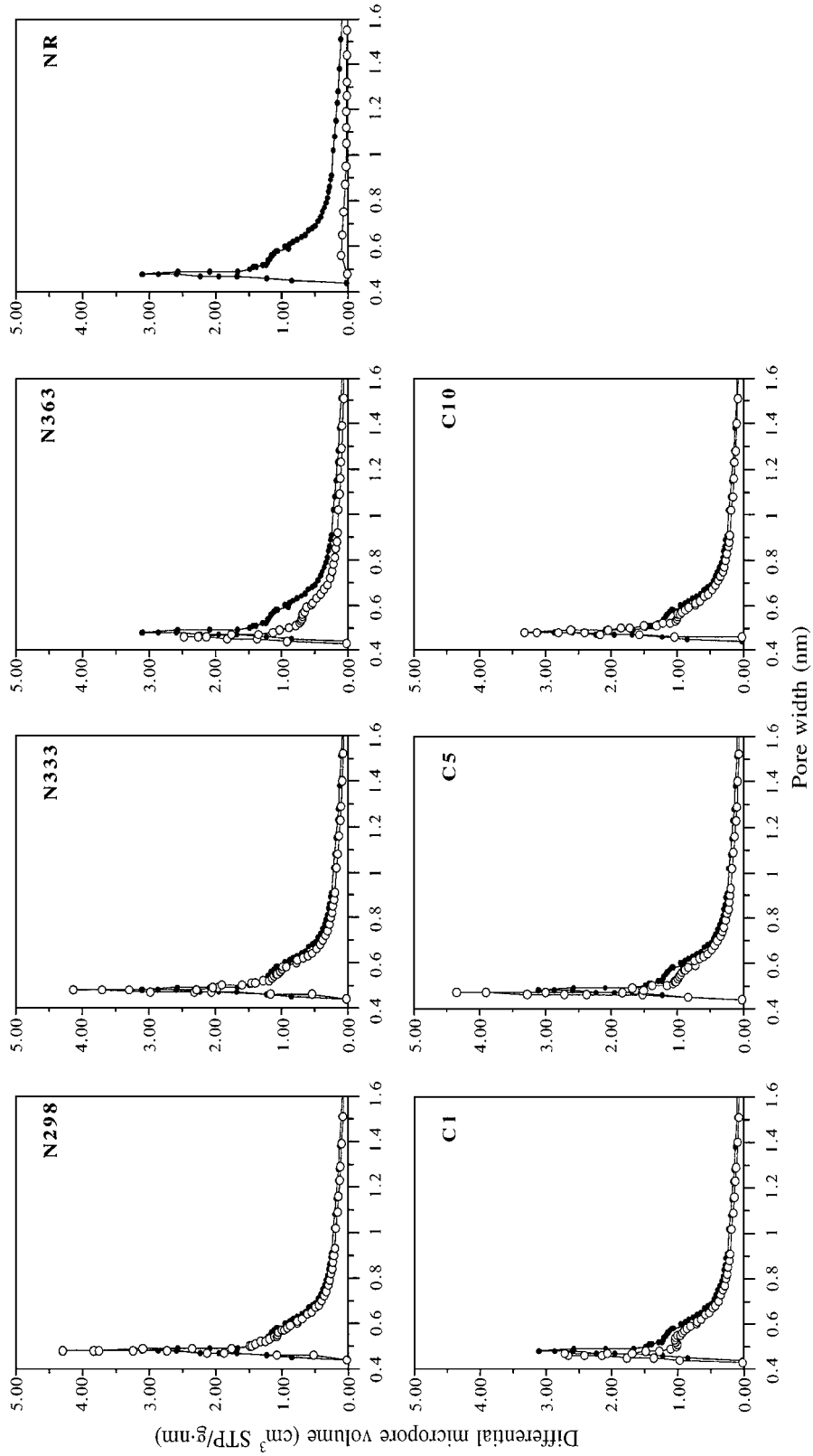

Figure 3. Micropore size distributions calculated from the Horvath-Kawazoe model of the activated carbons. (●) Starting activated carbon, (○) modified activated carbons.

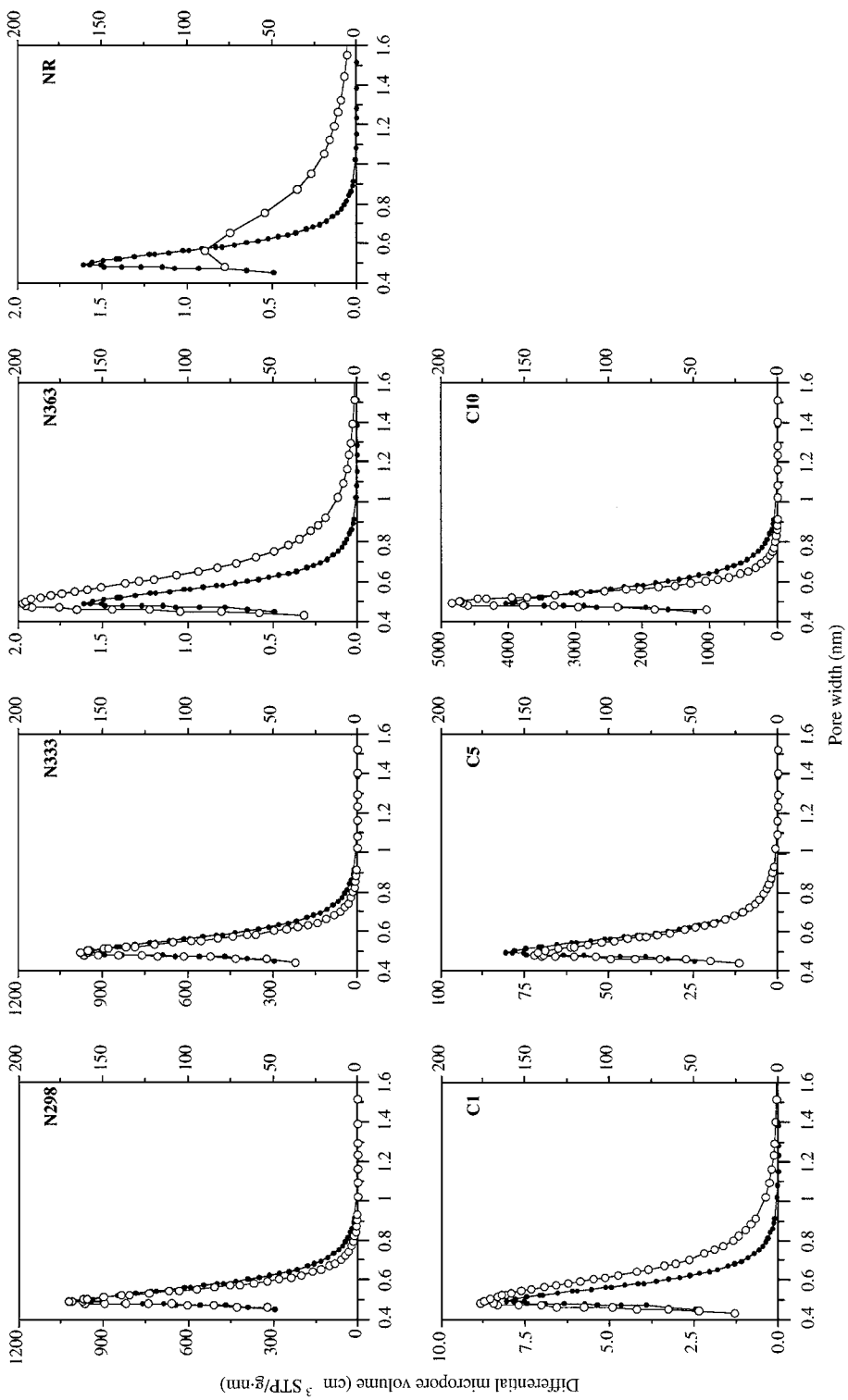

Figure 4. Micropore size distributions calculated from the Jaroniec-Gadkare-Choma model. (●) Starting activated carbon, right *Y*-axis (○) modified activated carbons, left *Y*-axis.

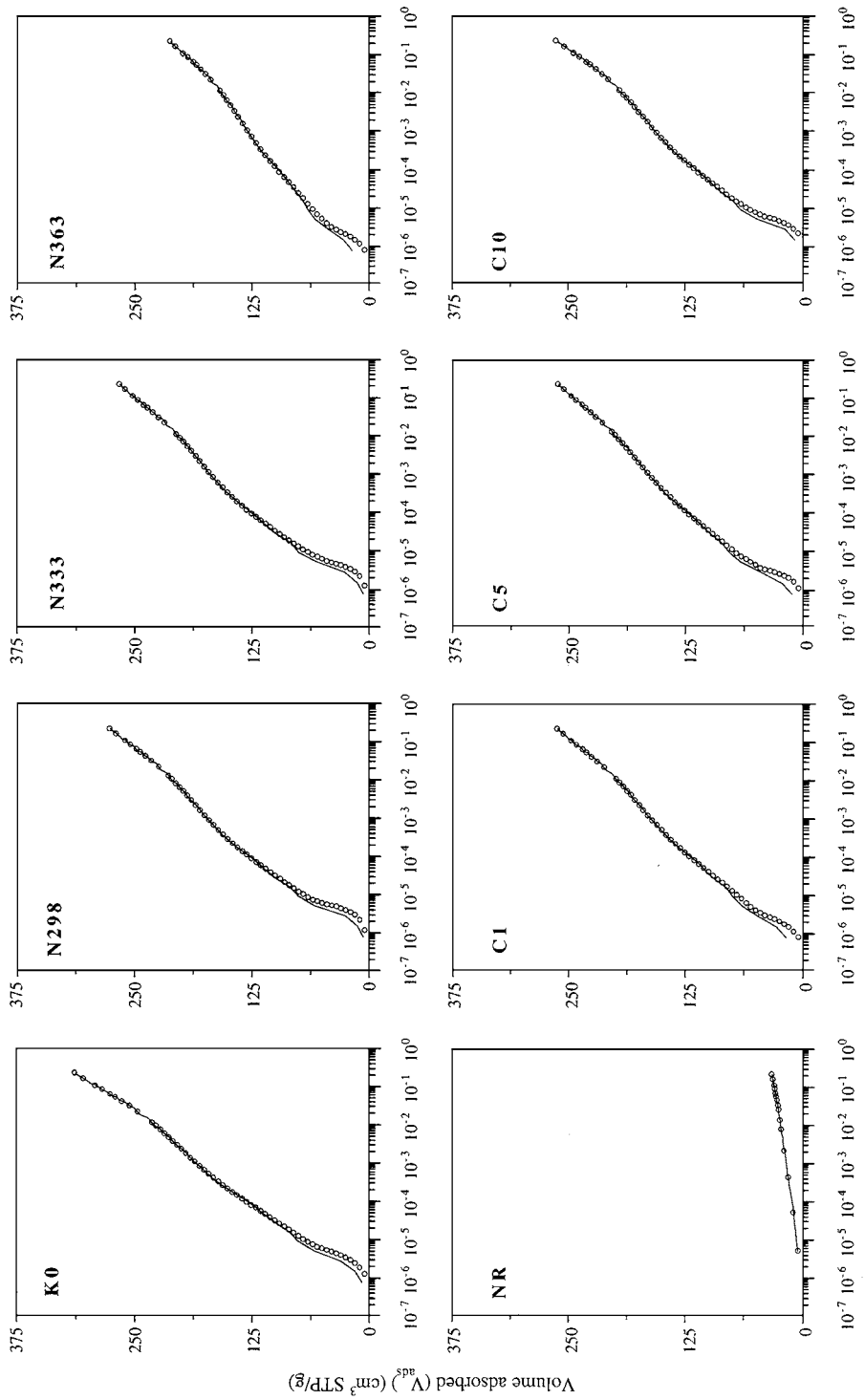

Figure 5. Nitrogen adsorption at 77 K up a relative pressure of 0.2. The density functional model (—) compared to experimental data (○).

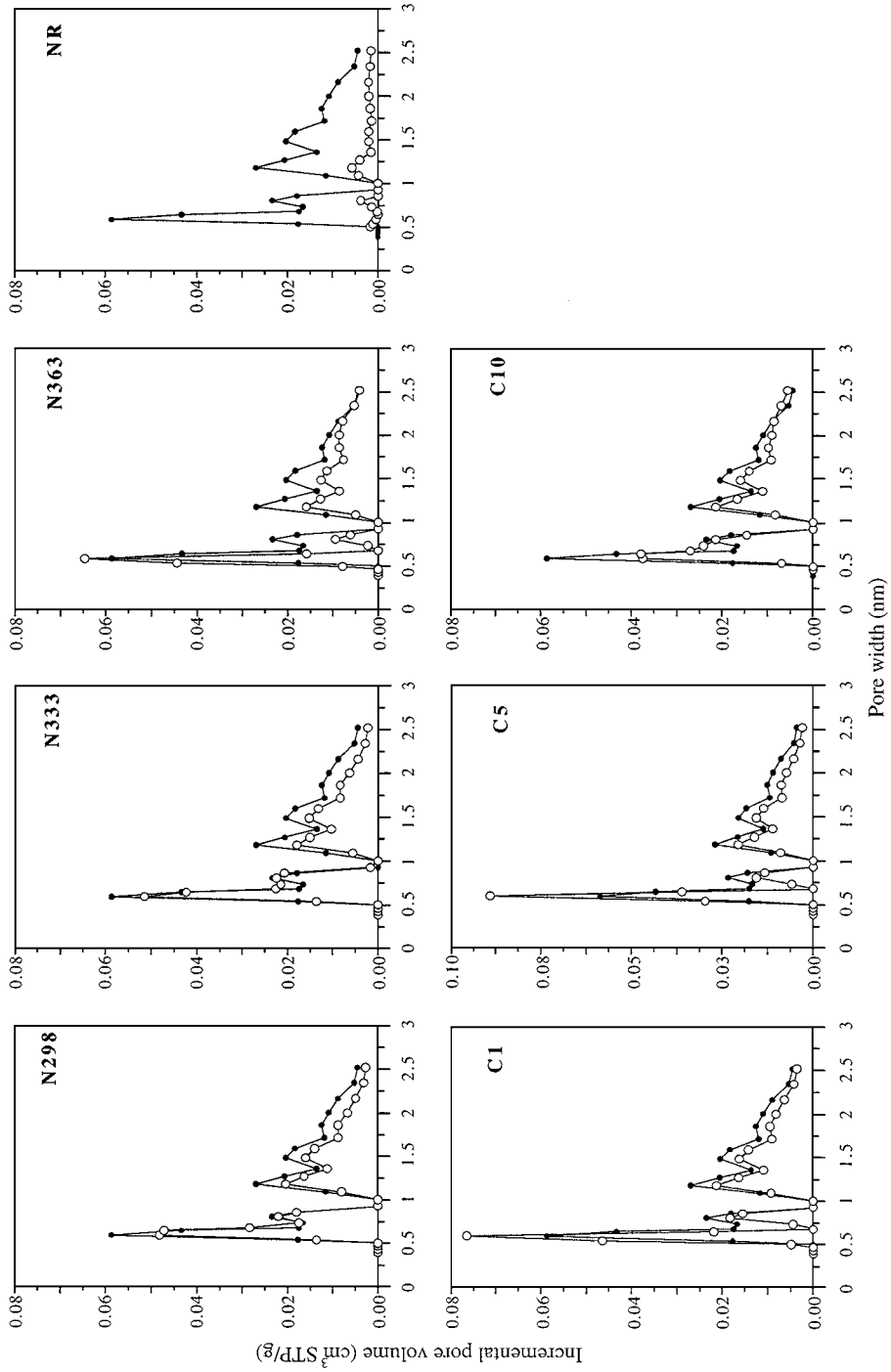

Figure 6. Micropore size distributions from the Density Functional Theory. (●) Starting activated carbon, (○) modified activated carbons.

the samples, only the relative intensity. The distribution curve for the NR sample shows a peak with a maximum located at about 0.56 nm.

In order to explain the uniformity of the results comparing HK and JGC models, the way the micropore size distributions are obtained must be taken into account. From a mathematical point of view, the two methods are identical. The only difference is in the sequence of calculations of micropore size distributions. In the HK method, the pressure scale of the adsorption isotherm is converted to the pore size scale using a theoretical relation between pressure and pore size and the resulting function is differentiated. In the JGC method, the pressure scale is converted to the adsorption potential, which is differentiated in order to obtain the adsorption potential distribution (Gil and Grange, 1997), and finally this distribution is multiplied by the differential $-dA/dx$ (see Eq. (11)). Thus, the second approach shows the relation between the adsorption potential distribution, which is a thermodynamic function, and the micropore size distribution, which depends on the model. The final results are very close, because the same pore geometry and the same relation between pressure and pore width are used.

The adsorption potential distributions of the samples have been presented elsewhere (Gil et al., 1997), in a study aiming to the investigation of the relation between the parameters of the DA equation and the distribution of the micropore widths. In that study, it can be seen that in fact there are differences among the adsorption potential distributions of the treated samples, mainly in their width. The distributions of the samples N298, N333 and C10 are sharper than the distribution of the starting activated carbon, while the ones for samples N363, NR, C1 and C5 are broader. These results indicate that the HNO_3 treatment produces an initial increase of the homogeneity of the microporous structure, but as the treatment temperature increases the structure becomes heterogeneous. The H_2O_2 treatment produces a heterogeneous structure that becomes homogeneous with the treatment concentration. When the adsorption potential distributions are multiplied by dA/dx to obtain the micropore size distributions, $J(x)$, the above variations between the adsorption potential distributions of the samples could explain the differences in relative intensity and width observed for the micropore size distributions from HK and JGC models.

The nitrogen adsorption isotherms up to a relative pressure of 0.2 obtained by the DFT model are shown in Fig. 5. The micropore size distributions $f(x)$ calculated from Eq. (14) for all samples are presented in Fig. 6. The corresponding adsorption characteristics are reported in Table 1. Only the nitrogen adsorption values up to a relative pressure of 0.2 were considered in applying the DFT model in order to relate adequately the relative pressure and the micropore size. If the whole relative pressure range is considered, a poor fitting of the adsorption values is obtained at very low pressures, modifying the micropore size distributions. At the distributions presented in Fig. 6, two micropore regions can be observed. In the case of small micropores, with widths below 1.0 nm, a bimodal distribution of pore sizes is obtained in all the samples, with sharp peaks at 0.59 and about 0.80 nm. For micropores wider than 1.0 nm, a broad pore size distribution is observed with also two maxima, at 1.18 and 1.48 nm. The microporous volumes, calculated as proposed by Gil and Grange (1997), were also included in Table 1. The discrepancies of the microporous volumes and the pore diameter maxima obtained from the distributions presented in Fig. 6, with respect to the values of the HK and DA approaches, must be related to the adsorbent-adsorbate properties used in this model (homotattic graphite (Olivier et al., 1994)). For illustrative purposes, the micropore size distributions of the KØ sample obtained from the HK model for the experimental nitrogen adsorption and for the simulated from the DFT model are presented in Fig. 7. These two distributions are similar enough, thus indicating that the discrepancies previously mentioned are due to the adsorbent-adsorbate properties.

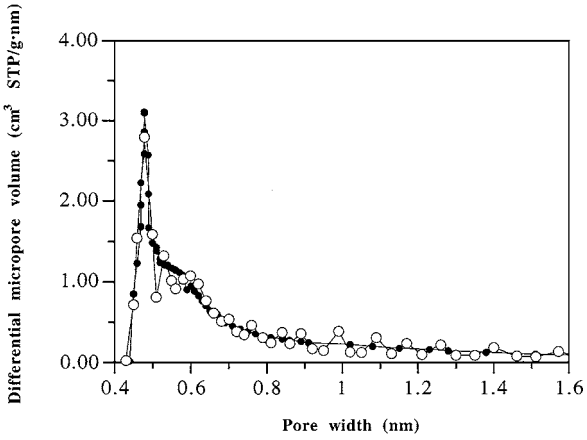

Figure 7. Micropore size distributions obtained from the HK model for the experimental (●) and the calculated (○) nitrogen adsorption isotherm from the DFT model.

5. Conclusions

Three methods, the Horvath-Kawazoe method, the Jaroniec-Gadkare-Choma one and the Density Functional Theory, have been applied to the nitrogen adsorption data obtained at 77 K in order to analyze the microporous structure of activated carbons, liquid-phase oxidized with HNO_3 and H_2O_2. Each method presented in this work can be applied to characterize the microporous properties of the modified activated carbon; however, there is a significant variation among the pore size distributions obtained. Besides, each method has a degree of uncertainty, and it is difficult to discern which is the most accurate. All equations contain several parameters, corresponding to physicochemical properties of the adsorbent and the adsorbate, which may be difficult to be estimated for some gas/solid systems. In the case of the HK method, an adequate value of the interaction parameter has been selected, in order to optimize the relative pressures that correspond to the micropore region.

The HK and the DFT methods describe satisfactorily the experimental results, including the transitions of the isotherms related to the stages of micropore filling. These methods qualitatively reproduce the form of the pore size distributions in the small micropore region, that is for micropores having widths below 1.0 nm. In the case of pores wider than 1.0 nm, DFT micropore size distribution exhibits two maxima at 1.18 and 1.48 nm. The JGC method also provides a satisfactory representation of adsorption in the present microporous systems.

Nomenclature

A	Adsorption potential, kJ/mol
A_a	Dispersion constant in Eqs. (1) and (2)
A_A	Dispersion constant in Eqs. (1) and (2)
c	Speed of light
C_1	Constant in Eqs. (12) and (13), kJ·nm/mol
C_2	Constant in Eqs. (12) and (13), nm^4
C_3	Constant in Eqs. (12) and (13), nm^{10}
C_4	Constant in Eqs. (12) and (13), nm
DFT	Density Functional Theory
d_a	Diameter of the adsorbent atom, nm
d_A	Diameter of the adsorbate molecule, nm
d_0	Arithmetic mean diameter of the adsorbate molecule and the adsorbent atom, nm
$d\mathrm{p}_{\mathrm{DFT}}$	Principal maximum pore diameter of the DFT pore size distribution, nm
$d\mathrm{p}_{\mathrm{HK}}$	Maximum pore diameter of the Horvath-Kawazoe micropore size distribution, nm
$d\mathrm{p}_{\mathrm{JGC}}$	Maximum pore diameter of the Jaroniec-Gadkare-Choma micropore size distribution, nm
E	Characteristic energy in the Dubinin-Astakhov equation, kJ/mol
$f(x)$	Pore size distribution, $cm^3/(g \cdot nm)$
$F(U)$	Differential distribution of pore volume (V) with respect to the adsorption energy (U), $(cm^3 \cdot mol)/(g \cdot kJ)$
G	Gibbs free energy, kJ/mol
HK	Horvath-Kawazoe model
JGC	Jaroniec-Gadkare-Choma model
$J(x)$	Differential distribution of pore volume (V) with respect to the pore width (x), $cm^3/(g \cdot nm)$
m	Electron mass
n	Exponent of the Dubinin-Astakhov equation
N_a	Number of oxide ions per unit area of surface
N_A	Number of molecules of adsorbate per unit surface area of adsorbate
N_{Av}	Avogadro's number
$N_aA_a + N_AA_A$	Interaction parameter, $cal \cdot nm^4/mol$
p	Pressure, Pa
p^0	Saturated vapor pressure of adsorbate, Pa
R	Universal gas constant, J/(mol·K)
S	Specific surface area, m^2/g
S_{ext}	Specific external surface area, m^2/g
S_{Lang}	Specific surface area from the Langmuir method, m^2/g
T	Temperature, K
U	Adsorption energy, kJ/mol
V	Specific pore volume, cm^3/g
V_{DA}	Specific micropore volume from Dubinin-Astakhov formalism, cm^3/g
$V_{\mu\mathrm{pDFT}}$	Specific micropore volume derived from the DFT model, cm^3/g
$V_{\mu\mathrm{pHK}}$	Specific micropore volume derived from the Horvath-Kawazoe model, cm^3/g
V_p	Specific total pore volume, cm^3/g
x	Pore width, nm
$X(A)$	Adsorption potential distribution, mol/kJ

$X(p)$	Experimental isotherm
z	Displacement of a molecule from the plane of surface nuclei

Greek Letters

α_a	Polarizability of an adsorbent atom, cm^3
α_A	Polarizability of an adsorbate molecule, cm^3
ΔG	Change in the Gibbs free energy, kJ/mol
ε	Potential energy of interaction, kJ/mol
σ	Constant in Eqs. (1) and (5), nm
$\varphi(p, x)$	Mean density of the adsorbate in a pore of width x at pressure p
χ_a	Magnetic susceptibility of an adsorbent atom, cm^3
χ_A	Magnetic susceptibility of an adsorbate molecule, cm^3

Acknowledgments

The authors thank Dr. G. de la Puente for the preparation of the samples.

References

Baksh, M.S.A. and R.T. Yang, "Model for Spherical Cavity Radii and Potential Functions of Sorbates in Zeolites," *AIChE J.*, **37**, 923–930 (1991).

Baksh, M.S.A. and R.T. Yang, "Unique Adsorption Properties and Potential Energy Profiles of Microporous Pillared Clays," *AIChE J.*, **38**, 1357–1368 (1992).

Bautista-Toledo, Y., J. Rivera-Utrilla, M.A. Ferro-Garcia, and C. Moreno-Castilla, "Influence of the Oxygen Surface Complexes of Activated Carbons on the Adsorption of Chromium Ions from Aqueous Solutions: Effect of Sodium Chloride and Humic Acid," *Carbon*, **32**, 93–100 (1994).

Brandt, K.B. and R.A. Kydd, "Characterization of Synthetic Microporous Pillared Beidellites of High Thermal Stability," *Chem. Mater.*, **9**, 567–572 (1997).

Cañizares, P., J.L. Valverde, M.R. Sun Kou, and C.B. Molina, "Synthesis and Characterization of PILCs with Single and Mixed Oxide Pillars Prepared from two Different Bentonites. A Comparative Study," *Microporous Mesoporous Mater.*, **28**, 267–281 (1999).

Carrot, P.J.M., R.A. Roberts, and K.S.W. Sing, "A New Method for the Determination of Micropore Size Distributions," in *Characterization of Porous Solids*, K.K. Unger, J. Rouquerol, K.S.W. Sing, and H. Kral (Eds.), pp. 89–100, Elsevier, Amsterdam, 1988.

Cheng, L.S. and R.T. Yang, "Improved Horvath-Kawazoe Equations including Spherical Pore Models for Calculating Micropore Size Distribution," *Chem. Eng. Sci.*, **49**, 2599–2609 (1994).

De Boer, J.H., B.G. Linsen, and Th.J. Osinga, "Studies on Pore Systems in Catalysts VI. The Universal t Curve," *J. Catal.*, **4**, 643–648 (1965).

De la Puente, G., A. Centeno, A. Gil, and P. Grange, "Interactions between Molybdenum and Activated Carbons on the Preparation of Activated Carbon-Supported Molybdenum Catalysts," *J. Colloid Interface Sci.*, **202**, 155–166 (1998).

De la Puente, G., A. Centeno, A. Gil, P. Grange, and B. Delmon, "Surface Functional Groups and Texture Characterisation of Catalytic Supports Based on Activated Carbon," in *Characterization of Porous Solids IV*, B. McEnaney, T.J. Mays, J. Rouquerol, F. Rodríguez-Reinoso, K.S.W. Sing, and K.K. Unger (Eds.), pp. 327–334, The Royal Society of Chemistry, Cambridge, 1997.

De la Puente, G., A. Gil, J.J. Pis, and P. Grange, "Effects of Support Surface Chemistry in Hydrodeoxygenation Reactions over CoMo/Activated Carbon Sulfided Catalysts," *Langmuir*, **15**, 5800–5806 (1999).

Derbysshire, F.J., V.H.J. de Beer, G.M.K. Abotsi, A.W. Scaroni, J.M. Solar, and D.J. Skrovanek, "The Influence of Surface Functionality on the Activity of Carbon-Supported Catalysts," *Appl. Catal.*, **27**, 117–131 (1986).

Do, H.D. and D.D. Do, "A Description of Adsorption in Activated Carbon Using a Hybrid Isotherm Equation," *Langmuir*, **11**, 2639–2647 (1995).

Dollimore, D. and G.R. Heal, "An Improved Method for the Calculation of Pore Size Distribution from Adsorption Data," *J. Appl. Chem.*, **14**, 109–114 (1964).

Dubinin, M.M., "Physical Adsorption of Gases and Vapors in Micropores," in *Progress in Surface and Membrane Science*, J.F. Danielli, M.D. Rosenberg, and D.A. Cadenhead, (Eds.), pp. 1–70, Academic Press, New York, 1975.

Ehrburger, P., O.P. Mahajan, and P.L. Walker, Jr., "Carbon as a Support for Catalysts I. Effect of Surface Heterogeneity of Carbon on Dispersion of Platinum," *J. Catal.*, **43**, 61–67 (1976).

Everett, D.H. and R.H. Ottewill, *Surface Area Determination*, Butterworths, London, 1970.

Everett, D.H. and J.C. Powl, "Adsorption in Slit-like and Cylindrical Micropores in the Henry's Law Region," *J. Chem. Soc., Faraday Trans. 1*, **72**, 619–636 (1976).

Foley, H.C., "Carbogenic Molecular Sieves: Synthesis, Properties and Applications," *Microporous Mater.*, **4**, 407–433 (1995).

Gandía, L.M. and M. Montes, "Effect of Thermal Treatments on the Properties of Nickel and Cobalt Activated Charcoal Supported Catalysts," *J. Catal.*, **145**, 267–288 (1994).

Ge, Z., D. Li, and T.J. Pinnavaia, "Preparation of Alumina-Pillared Montmorillonites With High Thermal Stability, Regular Microporosity and Lewis/Brönsted Acidity," *Microporous Mater.*, **3**, 165–175 (1994).

Gil, A. and P. Grange, "Application of the Dubinin-Radushkevich and Dubinin-Astakhov Equations in the Characterization of Microporous Solids," *Colloids and Surfaces A: Physicochemical and Engineering Aspects*, **113**, 39–50 (1996).

Gil, A. and P. Grange, "Comparison of the Microporous Properties of an Alumina Pillared Montmorillonite and an Activated Carbon from Nitrogen Adsorption at 77 K," *Langmuir*, **13**, 4483–4486 (1997).

Gil, A., G. de la Puente, and P. Grange, "Evidence of Textural Modifications of an Activated Carbon on Liquid-Phase Oxidation Treatments," *Microporous Mater.*, **12**, 51–61 (1997).

Gil, A. and S.A. Korili, "Structural Heterogeneity of Microporous Materials from Nitrogen Adsorption at 77 K," *Bol. Soc. Esp. Ceram. Vid.*, **39**, 35–39 (2000).

Gil, A., A. Massinon, and P. Grange, "Analysis and Comparison of the Microporosity in Al-, Zr-, and Ti-Pillared Clays," *Microporous Mater.*, **4**, 369–378 (1995).

Gil, A. and M. Montes, "Analysis of the Microporosity in Pillared Clays," *Langmuir*, **10**, 291–297 (1994).

Gil, A., M.A. Vicente, and L.M. Gandía, "Main Factors Controlling the Texture of Zirconia and Alumina Pillared Clays," *Microporous Mesoporous Mater.*, **34**, 115–125 (2000).

Gregg, S.J. and K.S.W. Sing, *Adsorption, Surface Area and Porosity*, Academic Press, London, 1991.

Heuchel, M. and M. Jaroniec, "Comparison of Energy Distributions Calculated for Active Carbons from Benzene Gas/Solid and Liquid/Solid Adsorption Data," *Langmuir*, **11**, 1297–1303 (1995a).

Heuchel, M. and M. Jaroniec, "Use of Simulated Adsorption Isotherms to Study Surface and Structural Heterogeneities of Microporous Solids," *Langmuir*, **11**, 4532–4538 (1995b).

Horvath, G. and K. Kawazoe, "Method for the Calculation of Effective Pore Size. Distribution in Molecular Sieve Carbon," *J. Chem. Eng. Jpn.*, **16**, 470–475 (1983).

Hutson, N.D., M.J. Hoekstra, and R.T. Yang, "Control of Microporosity of Al_2O_3-Pillared Clays: Effect of pH, Calcination Temperature and Clay Cation Exchange Capacity," *Microporous Mesoporous Mater.*, **28**, 447–459 (1999).

Jagiello, J. and J.A. Schwarz, "Relationship between Energetic and Structural Heterogeneity of Microporous Carbons Determined on the Basis of Adsorption Potentials in Model Micropores," *Langmuir*, **9**, 2513–2517 (1993).

Jaroniec, M., "Characterization of Nanoporous Materials," in *Access to Nanoporous Materials*, T.J. Pinnavaia and M. Thorpe (Eds.), pp. 255–272, Plenum Press, New York, 1995.

Jaroniec, M. and J. Choma, "On the Characterization of Structural Heterogeneity of Microporous Solids by Discrete and Continous Micropore Distribution Functions," *Mater. Chem. Phys.*, **19**, 267–289 (1988).

Jaroniec, M., J. Choma, A. Swiatkowski, and K.H. Radeke, "Application of Isotherm Equation Associated with Gamma Micropore-Size Distribution for Characterizing Activated Carbons," *Chem. Eng. Sci.*, **43**, 3151–3156 (1988).

Jaroniec, M., K.P. Gadkaree, and J. Choma, "Relation between Adsorption Potential Distribution and Pore Volume Distribution for Microporous Carbons," *Colloids and Surface A: Physicochemical and Engineering Aspects*, **118**, 203–210 (1996).

Jaroniec, M., R.K. Gilpin, K. Kaneko, and J. Choma, "Evaluation of Energetic Heterogeneity and Microporosity of Activated Carbon Fibers on the Basis of Gas Adsorption Isotherms," *Langmuir*, **7**, 2719–2722 (1991).

Jaroniec, M. and K. Kaneko, "Physicochemical Foundations for Characterization of Adsorbents by Using High-Resolution Comparative Plots," *Langmuir*, **13**, 6589–6596 (1997).

Jaroniec, M. and R. Madey, *Physical Adsorption on Heterogeneous Solids*, Elsevier, Amsterdam, 1988.

Jaroniec, M., R. Madey, J. Choma, B. McEnaney, and T.J. Mays, "Comparison of Adsorption Methods for Characterizing the Microporosity of Activated Carbons," *Carbon*, **27**, 77–83 (1989).

Kakei, K., S. Ozeki, T. Suzuki, and K. Kaneko, "Multi-Stage Micropore Filling Mechanism of Nitrogen on Microporous and Micrographitic Carbons," *J. Chem. Soc., Faraday Trans.*, **86**, 371–376 (1990).

Kim, K.T., Y.G. Kim, and J.S. Chung, "Adsorption of Cationic Platinum Complex onto Carbon Support," *Carbon*, **31**, 1289–1296 (1993).

Kruk, M., M. Jaroniec, and J. Choma, "Critical Discussion of Simple Adsorption Methods used to Evaluate the Micropore Size Distribution," *Adsorption*, **3**, 209–219 (1997).

Kruk, M., M. Jaroniec, and J. Choma, "Comparative Analysis of Simple and Advanced Sorption Methods for Assessment of Microporosity in Activated Carbons," *Carbon*, **36**, 1447–1458 (1998).

Lastoskie, C., K.E. Gubbins, and N. Quirke, "Pore Size Heterogeneity and the Carbon Slit Pore: A Density Functional Theory Model," *Langmuir*, **9**, 2693–2702 (1993a).

Lastoskie, C., K.E. Gubbins, and N. Quirke, "Pore Size Distribution Analysis of Microporous Carbons," *J. Phys. Chem.*, **97**, 4786–4796 (1993b).

Lecloux, A. and J.P. Pirard, "The Importance of Standard Isotherms in the Analysis of Adsorption Isotherms for Determining the Porous Texture of Solids," *J. Colloid Interface Sci.*, **70**, 265–281 (1979).

Lippens, B.C. and J.H. de Boer, "Studies on Pore Systems in Catalysts V. The t Method," *J. Catal.*, **4**, 319–323 (1965).

Malla, P.B. and S. Komarneni, "Properties and Characterization of Al_2O_3 and SiO_2-TiO_2 Pillared Saponite," *Clays Clay Miner.*, **41**, 472–483 (1993).

Martín-Gullón, A., C. Prado-Burguete, and F. Rodríguez-Reinoso, "Effect of Carbon Properties on the Preparation and Activity of Carbon-Supported Molybdenum Sulfide Catalysts," *Carbon*, **31**, 1099–1105 (1993).

Mikhail, R.Sh., S. Brunauer, and E.E. Bodor, "Capillary Condensation and Pore Structure Analysis," *J. Colloid. Interface Sci.*, **26**, 45–60 (1968).

Nicholson, D. "Simulation Study of Nitrogen Adsorption in Parallel-Sided Micropores with Corrugated Potential Functions," *J. Chem. Soc., Faraday Trans.*, **90**, 181–185 (1994).

Olivier, J.P., W.B. Couklin, and M. von Szombathel, "Determination of Pore Size Distributions from the Density Functional Theory," *Stud. Surf. Sci. Catal.*, **87**, 81–89 (1994).

Parent, M.A. and J.B. Moffat, "A Comparison of Methods for the Analysis of Adsorption-Desorption Isotherms of Microporous Solids," *Langmuir*, **11**, 4474–4479 (1995).

Prado-Burguete, C., A. Linares-Solano, F. Rodríguez-Reinoso, and C. Salinas-Martínez de Lecea, "The Effect of Oxygen Surface Groups of the Support on Platinum Dispersion in Pt/Carbon Catalysts," *J. Catal.*, **115**, 98–106 (1989).

Prado-Burguete, C., A. Linares-Solano, F. Rodríguez-Reinoso, and C. Salinas-Martínez de Lecea, "Effect of Carbon Support and Mean Pt Particle Size on Hydrogen Chemisorption by Carbon-Supported Pt Catalysts," *J. Catal.*, **128**, 397–404 (1991).

Puri, B.R. "Surface Complexes on Carbons," in *Chemistry and Physics of Carbon*, P.L. Walker, Jr. (Ed.), pp. 191–282, Marcel Dekker, New York, 1970.

Román-Martínez, M.C., D. Cazorla-Amorós, A. Linares-Solano, C. Salinas-Martínez de Lecea, H. Yamashita, and M. Anpo, "Metal-Support Interaction in Pt/C Catalysts. Influence of the Support Surface Chemistry and the Metal Precursor," *Carbon*, **33**, 3–13 (1995).

Ross, S. and J.P. Olivier, *On Physical Adsorption*, Wiley, New York, 1964.

Russell, B.P. and M.D. LeVan, "Pore Size Distribution of BPL Activated Carbon Determined by Different Methods," *Carbon*, **32**, 845–855 (1994).

Rychlicki, G., A.P. Terzyk, and G.S. Szymánski, "The Effect of Carbon Surface Modification on its Microporous Structure. Application of Horvath-Kawazoe Method for the Calculation of Effective Pore Size Distribution," *Polish J. Chem.*, **67**, 2029–2035 (1993).

Saito, A. and H.C. Foley, "Curvature and Parametric Sensitivity in Models for Adsorption in Micropores," *AIChE J.*, **37**, 429–436 (1991).

Saito, A. and H.C. Foley, "Argon Porosimetry of Selected Molecular Sieves: Experiments and Examination of the Adapted Horvath-Kawazoe Model," *Microporous Mater.*, **3**, 531–542 (1995a).

Saito, A. and H.C. Foley, "High-Resolution Nitrogen and Argon Adsorption on ZSM-5 Zeolites: Effects of Cation Exchange and Si/Al Ratio," *Microporous Mater.*, **3**, 543–556 (1995b).

Seaton, N.A., J.P.R.B. Walton, and N. Quirke, "A New Analysis Method for the Determination of the Pore Size Distribution of Porous Carbons from Nitrogen Adsorption Measurements," *Carbon*, **27**, 853–861 (1989).

Sing, K.S.W., "The Use of Physisorption for the Characterization of Microporous Carbons," *Carbon*, **27**, 5–11 (1989).

Stoeckli, H.F., "A Generalization of the Dubinin-Radushkevich Equation for the Filling of Heterogeneous Micropore Systems," *J. Colloid Interface Sci.*, **59**, 184–185 (1977).

Storaro, L., M. Lenarda, R. Ganzerla, and A. Rinaldi, "Preparation of Hydroxy Al and Al/Fe Pillared Bentonites from Concentrated Clay Suspensions," *Microporous Mater.*, **6**, 55–63 (1996).

Suh, D.J., T.-J. Park, and S.-K. Ihm, "Effect of Surface Oxygen Groups of Carbon Supports on the Characteristics of Pd/C Catalysts," *Carbon*, **31**, 427–435 (1993).

Suzuki, T., K. Kaneko, N. Setoyama, M. Maddox, and K. Gubbins, "Grand Canonical Monte Carlo Simulation for Nitrogen Adsorption in Graphitic Slit Micropores: Effect of Interlayer Distance," *Carbon*, **34**, 909–912 (1996).

Vissers, J.P.R., S.M.A.M. Bouwens, V.J.H. de Beer, and R. Prins, "Carbon Black-Supported Molybdenum Sulfide Catalysts," *Carbon*, **25**, 485–493 (1987).

Webb, P.A. and C. Orr, "Adsorption, Analytical Methods in Fine Particle Technology," Micromeritics Instrument Corp., pp. 53–153, Norcross, 1997.

Zhu, H.Y., G.Q. Lu, N. Maes, and E.F. Vansant, "Pore Structure Characterisation of Pillared Clays Using a Modified MP Method," *J. Chem. Soc., Faraday Trans.*, **93**, 1417–1423 (1997).